Medical Engineering & Physics 34 (2012) 1177–1183

Contents lists available at SciVerse ScienceDirect

Medical Engineering & Physics

journal homepage: www.elsevier.com/locate/medengphy

Computational analysis of the flow of bile in human cystic duct

Mushtak Al-Atabi[a,*], R.C. Ooi[b,1], X.Y. Luo[c,2], S.B. Chin[b,1], N.C. Bird[d,3]

[a] School of Engineering, Taylor's University, No 1 Jalan Taylor's, 47500 Subang Jaya, Selangor, Malaysia
[b] Department of Mechanical Engineering, The University of Sheffield, Mappin Street, Sheffield S1 3JD, United Kingdom
[c] School of Mathematics and Statistics, University of Glasgow, University Gardens, Glasgow G12 8QW, United Kingdom
[d] Academic Surgical Unit, Royal Hallamshire Hospital, Sheffield S10 2JF, United Kingdom

ARTICLE INFO

Article history:
Received 7 October 2011
Received in revised form 5 December 2011
Accepted 8 December 2011

Keywords:
Cystic duct
Biliary system
Bile flow
Gallstones
Computational fluid dynamics

ABSTRACT

Computational fluid dynamic (CFD) simulations of the three-dimensional flow structures in realistic cystic ducts have been performed to obtain quantitative readings of the flow parameters to compare with clinical measurements. Resin casts of real patients' cystic ducts lumen that possess representative anatomical features were scanned to obtain three-dimensional flow domains that were used in the numerical analysis. The convoluting nature of the studied cystic ducts resulted in strong secondary flow that contributed towards a dimensionless pressure drop that is four times higher than those of a straight circular tube of an equivalent length and average diameter. The numerical pressure drop results across the cystic duct compared very well with those obtained from clinical observations which indicate that CFD is an appropriate tool to investigate the flow and functions of the biliary system. From the hydrodynamic point of view, the cystic duct lumen seems to serve as a passive resistor that strives to provide a constant amount of resistance to control the flow of bile out of the gallbladder. This is mainly achieved by the coupling of the secondary flow effects and bile rheology to provide flow resistance.

1. Introduction

The human biliary system is responsible for creating, transporting, storing and releasing bile into the duodenum to aid digestion of fats [1]. The anatomy of the biliary system is shown in Fig. 1. Bile is continuously secreted by the liver, transported via the common hepatic duct and cystic duct and stored in the gallbladder until it is needed [2]. During meals, cholecystokinin (CCK) hormones are released into the blood supplying the biliary system to stimulate gallbladder contraction and relax the sphincter of Oddi [3]. The bile is expelled from the gallbladder and flows through the cystic duct to the common bile duct and released into the duodenum.

Although seldom life threatening, treatment of gallstone related diseases represents an estimated annual cost of $5 billion in the United States and £60 million [4] to the National Health Service in the United Kingdom.

While the presence of gallstones is normally attributed to supersaturation of bile with cholesterol and the presence of calculi nucleating agents in it, Ref. [5] showed that supersaturated bile frequently exists in healthy individuals indicating that stasis of bile within the gallbladder may be an important factor in the formation of gallstones.

Nomenclature

D	diameter (m)
D_h	hydraulic diameter (m)
L	length (m)
P	static pressure (cmH_2O, Pa)
Q	volumetric flow rate ($m^3\,s^{-1}$)
u	fluid velocity tensor ($m\,s^{-1}$)
U	mean fluid velocity ($m\,s^{-1}$)
V	volume (m^3)
ΔP	pressure drop (cmH_2O, Pa)
Λ	dimensionless pressure, $(\rho D^2\,\Delta P/\mu^2)/(L/D)$
ρ	fluid density ($kg\,m^{-3}$)
μ	dynamic viscosity ($N\,s\,m^{-2}$)

Dimensionless numbers

Cp	pressure coefficient, Euler number $2\,\Delta P/\rho U^2$
f	friction factor $Cp/(L/D)$
Re	Reynolds number, $\rho UD/\mu$

* Corresponding author. Tel.: +60 356295451; fax: +60 356295477.
E-mail addresses: mushtak.t@taylors.edu.my (M. Al-Atabi), xiaoyu.luo@glasgow.ac.uk (X.Y. Luo), S.B.Chin@shef.ac.uk (S.B. Chin), N.Bird@shef.ac.uk (N.C. Bird).
[1] Tel.: +44 114 222 7735; fax: +44 114 222 7890.
[2] Tel.: +44 141 330 5176; fax: +44 141 330 4111.
[3] Tel.: +44 114 226 8018; fax: +44 114 271 3791.

1350-4533/$ – see front matter © 2011 IPEM. Published by Elsevier Ltd. All rights reserved.
doi:10.1016/j.medengphy.2011.12.006

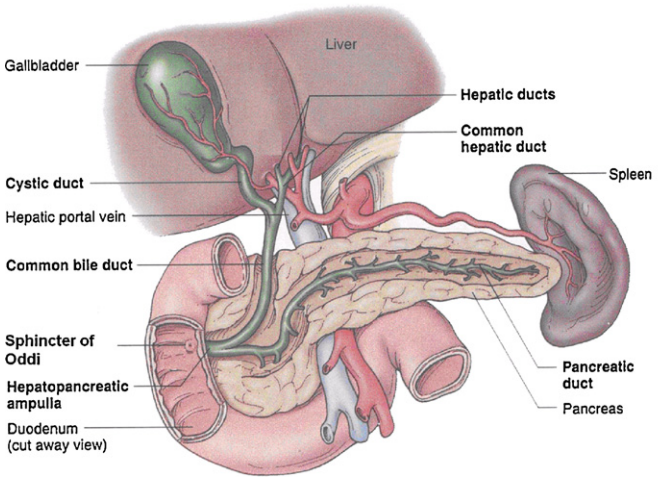

Fig. 1. Gross anatomy of the human biliary system.

Further studies on gallstone and gallbladder diseases have suggested that fluid mechanics of the biliary system may be a contributing factor in the pathogenesis of gallbladder diseases [6–8]. Ooi et al. [2] employed computational fluid dynamics (CFD) modelling, using steady flow and rigid wall assumptions in both idealised and realistic cystic duct models. Al-Atabi et al. [9–13] experimentally investigated the flow of bile in idealised three-dimensional and realistic two-dimensional cystic duct geometries. The effects of the compliance of the cystic ducts and non-Newtonian properties of the bile on biliary resistance are studied by Li et al. [14,15] using both one-dimensional and idealised three-dimensional mathematical models. Recently, these models are further extended to identify the correlation of mechanical stress of gallbladder wall to CCK induced pain [16], as well as the smooth muscle contractions [17]. These works have demonstrated that non-invasive mathematical models can be developed to drive our understanding of gallbladder diseases.

The objective of this study is to investigate the flow patterns in real cystic duct geometries during the gallbladder emptying cycle using computational fluid dynamics (CFD) techniques. This aimed at generating quantitative results for the bile flow parameters to be compared with the clinical results often obtained from X-rays in order to further understand the role of bile flow phenomenon and the geometry of cystic duct in how it controls the bile flow.

2. Clinical background

The geometry of the cystic duct is complex and varies from one individual to another. The cystic duct diameter and length range from 2 to 5 mm and 10 to 60 mm, respectively [2]. Heister [18] described the presence of folds in the cystic duct, later termed "valves of Heister". Mentzer [19] had observed what he called "leaflets" in the lumen of the duct after incising it longitudinally. He went on to describe instances where several "leaflets" joined to form spiral "valves," a description also used by Lichtenstein and Ivy [20]. In this study, computational fluid dynamics (CFD) is used to study the flow in cystic ducts. The computational models are constructed based on real cystic ducts that are surgically removed during routine cholecystectomy.

2.1. Cystic duct anatomy

The lumen of the cystic duct is complicated and its effective geometry can be further modified by the presence of the mucus layer. In order to capture the internal anatomic details of the cystic ducts, a two-part resin (Scott Bader, Strand, UK) was injected into the ducts to create solid casts. Once the resin cured, cystic duct tissue was removed exposing the solid casts. Thirty-seven resin casts were studied and the prominent geometrical features in these cases were found to be helical (48.6%), corrugated (51.4%) and kinked (10.8%) conduits [21]. These casts are assigned three-digit identification numbers (Castxxx). Two casts (Cast010 and Cast034) with representative lumen structures were selected (Fig. 2) and scanned using the Model Maker W (3D Scanners, UK) for their 3D geometry profiles. The geometries were then exported into the software GAMBIT [22] to set up the mesh for CFD calculations.

Cast010 was obtained from a gallstone patient. The gallbladder neck was bent at a 90° angle and the lumen was corrugated. Cast034 was reconstructed from a partial hepatectomy (liver removal) patient. The gallbladder neck portion was S-like (Hartmann's pouch) and spirals into the helical cystic duct conduit. The basic dimensions including the hydraulic diameter at cystic duct inlets, D_h, were tabulated in Table 1.

2.2. Flow assumptions

Human gallbladder empties at an average rate of 1 ml/min with a maximum flow rate of 5 ml/min as suggested by ultrasonographic imaging of the rate of change of the gallbladder volume [23]. The average flow rate in the cystic duct is about 0.5–1.0 ml/min for fasting gallbladders and 2.0–3.0 ml/min after meal [24]. The Reynolds number, *Re*, based on mean velocity and mean duct diameter, thus varies from 1 to 40. In addition, as the average time to empty a gallbladder with a mean volume of 35 ml of bile is about 30 min [25], this study assumes that the flow is laminar and that it is sufficiently slow changing to consider that steady state conditions prevail.

Although a literature search reveals that there are few convincing rheological data on human bile, preliminary measurements of fresh bile and preliminary modelling [15] suggest that for a healthy person without gallstones, the gallbladder and hepatic bile is a Newtonian fluid with a constant viscosity of about 1–10 mPa s and a density of nearly 1000 kg m^{-3}. These values for density and viscosity will be used in this study.

Although the walls of cystic ducts have some muscle tissues, it is still to be established if the cystic duct or its muscular tissue plays a dominant role in controlling the flow of bile [21] and hence the cystic duct walls will be considered to be rigid for the purpose of this study.

Table 1
Geometrical details of the two casts used in this study.

Cast	Section	Perimeter (m)	Area (m^2)	D_h (m)	L (m)	L/D_h	Boundary condition
010	Gallbladder inlet	2.08E−2	3.09E−5	–	–	–	Inlet velocity
	Cystic duct inlet	1.07E−2	6.93E−6	2.60E−3	1.93E−2	7.43	Interior
	Cystic duct outlet	7.53E−3	4.41E−6	–	–	–	Pressure outlet
034	Gallbladder inlet	1.83E−2	2.54E−5	–	–	–	Inlet velocity
	Cystic duct inlet	6.79E−3	3.57E−6	2.10E−3	1.12E−2	5.33	Interior
	Cystic duct outlet	4.53E−3	1.49E−6	–	–	–	Pressure outlet

L: cystic duct length; D_h: hydraulic diameter (4 × area/perimeter).

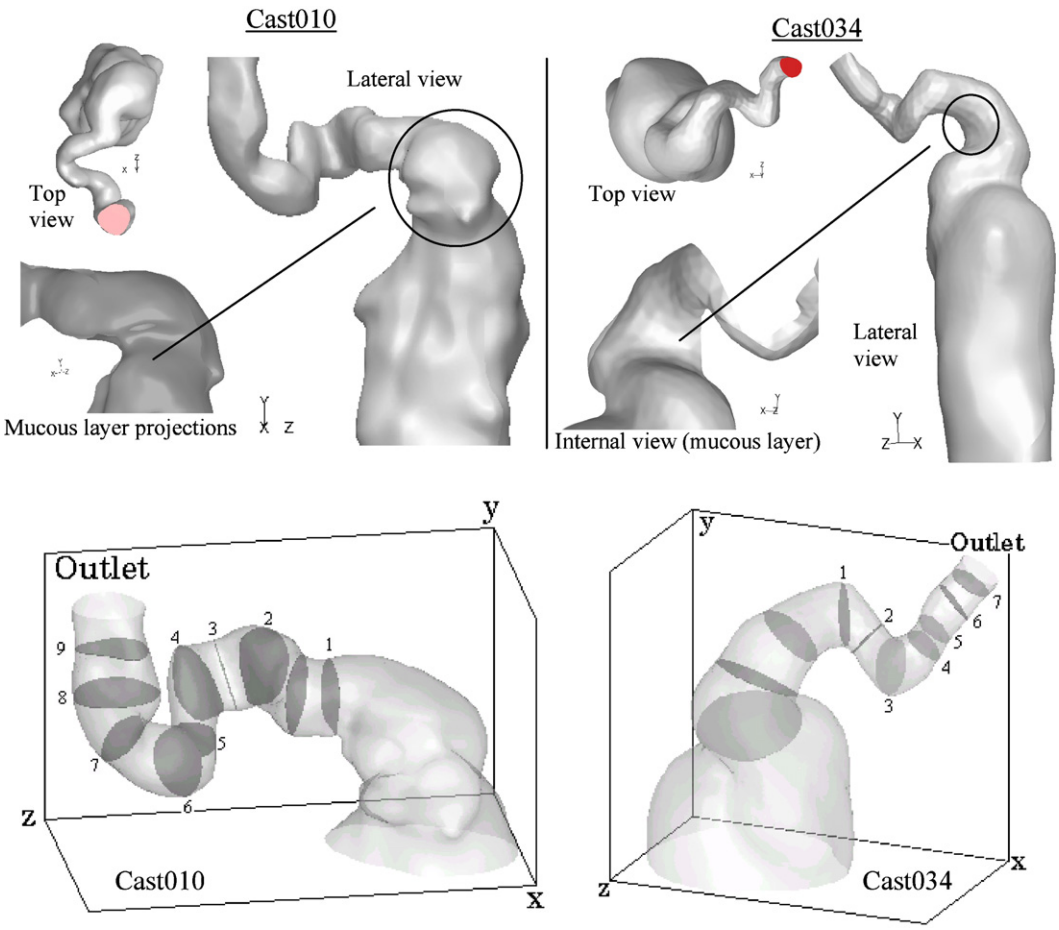

Fig. 2. Scanned 3D lumen geometry from resin casts (gallbladder neck circled) and numbered planes for flow visualisation.

2.3. Fluid pressure in the biliary system

The two main sources of pressure in the biliary tree are the liver and the gallbladder, which is the only dynamic organ in the biliary system. The maximum liver secretion pressure is approximately 30 cmH_2O (2942 Pa) [26], while the human gallbladder has a resting pressure of around 10–20 cmH_2O (980–1960 Pa) and requires a pressure head of only a few centimetres of water to empty the bile to the common bile duct [25]. Continuous in vivo manometry of human gallbladder showed that, after a meal, the pressure in the gallbladder increases to around 26.2–38.7 cmH_2O (2569–3795 Pa). The pressure in the common bile duct is around 5–10 cmH_2O (490–980 Pa) above the duodenal pressure [25]. When given a meal or exogenous doses of cholecystokinin (CCK-8), the human gallbladder pressure can rise up to about 40 cmH_2O (3920 Pa). The common bile duct pressure will also change from 10 to 19 cmH_2O (980–1863 Pa) [27,28].

Since the cystic duct is a bi-directional conduit, the pressure difference across it dictates not only the flow rate of the bile but the direction of the flow as well. Early in vitro studies employed manometers to quantify the pressure drop across the cystic duct. These studies showed that the pressure difference needed to initiate the flow of bile in the cystic duct varied from 0.1 cmH_2O (9.8 Pa) [20] to 8 cmH_2O (785 Pa) [29]. This large difference can be, at least in part, attributed to the variation in the geometry of the cystic duct which plays an important role in the pressure drop across it. Since the 1980s, biliary pressures were measured with catheters perfused with a constant flow of solution and computerised recording devices for data collection. The method was further modified by using pressure micro-transducers that can be placed at bile duct in vivo [28,30]. Such arrangement allows the detection of how the gallbladder contractions changes biliary duct pressures.

3. Numerical solution

The flow assumptions mentioned above reduce the continuity equation and the Navier-Stokes equation to the forms given by Eqs. (1) and (2), respectively:

$$\frac{\partial u_i}{\partial x_i} = 0 \tag{1}$$

$$u_j \frac{\partial u_i}{\partial x_j} = \nu \nabla^2 u_i - \frac{1}{\rho} \frac{\partial P}{\partial x_i} \tag{2}$$

These flow equations are solved using the finite volume based computational fluid dynamics (CFD) package Fluent6.1 [22]. For the steady, incompressible laminar bile flow, a pressure-correction type algorithm, SIMPLE-C, was employed to solve continuity and momentum equations sequentially. Under this method, non-linear governing equations are linearised to produce a system of equations for the dependent variables in every computational cell. The resultant linear system is then solved to yield an updated flow-field solution. A point implicit (Gauss–Seidel) linear equation solver is used in conjunction with an algebraic multigrid (AMG) method to solve the resultant system of equations for the dependent variable in each cell.

The 3D cast models contain details of part of the gallbladder body until the distal part of the cystic duct. Both the gallbladder

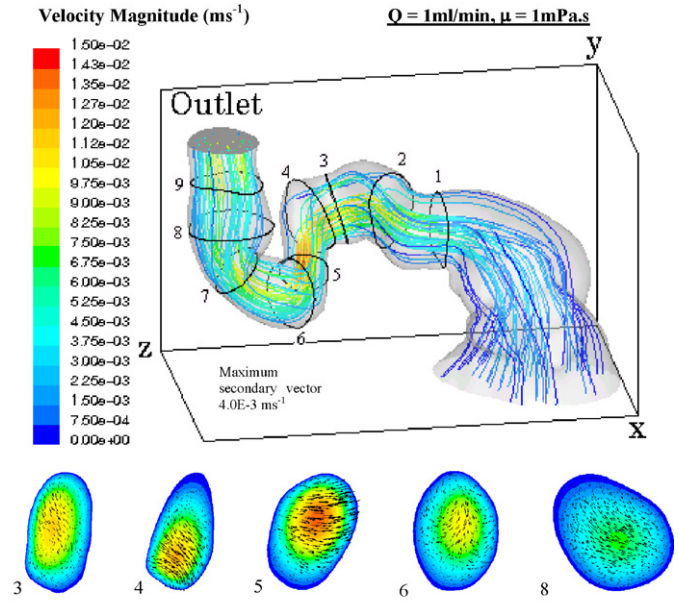

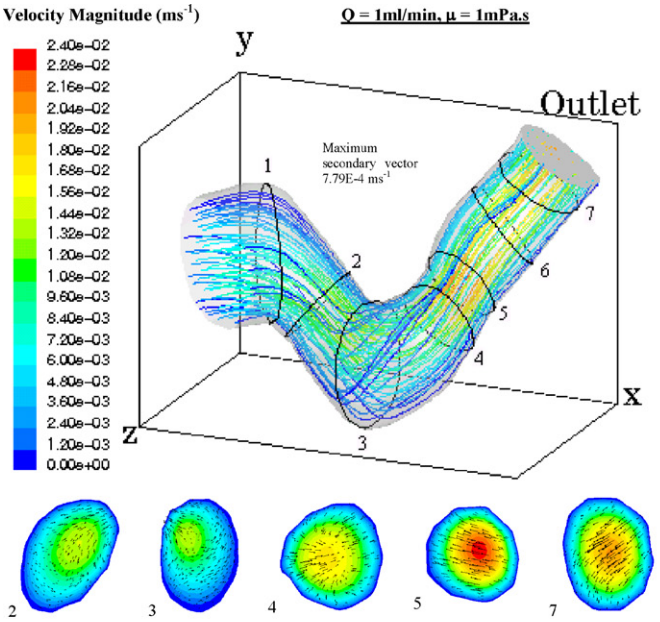

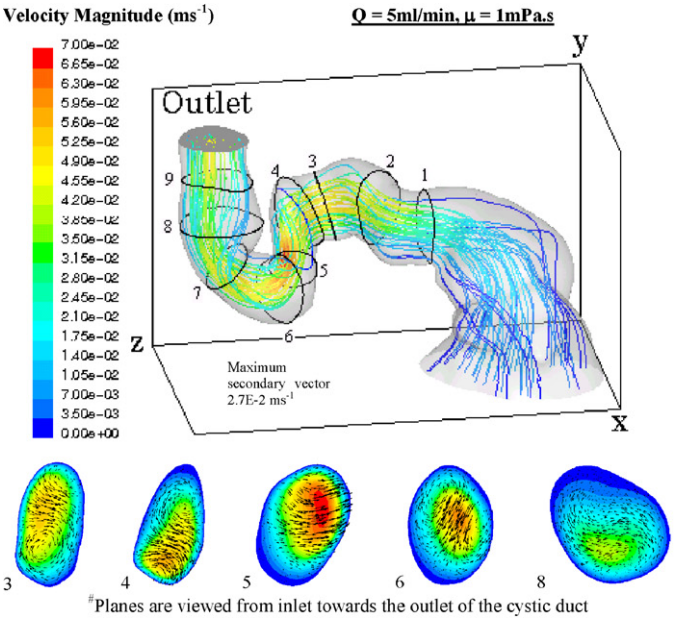

Fig. 3. Path lines coloured by velocity magnitude ($m\,s^{-1}$) contour and secondary velocity vector plots for Cast010.

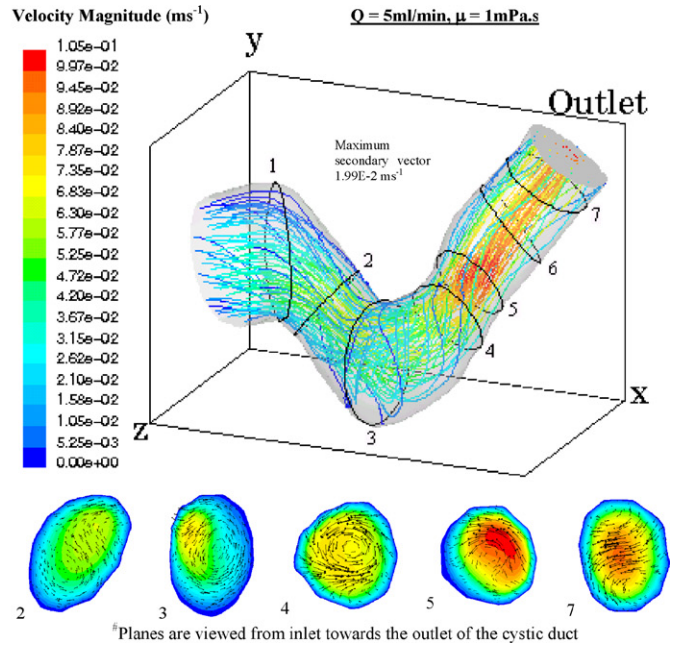

Fig. 4. Path lines coloured by velocity magnitude ($m\,s^{-1}$) contour and secondary velocity vector plots in Cast034.

inlet section and the cystic duct outlet have irregular shapes and flow rate range between 0.1 and 10 ml/min were employed across them to measure the static pressure drop. Boundary conditions employed were summarised in Table 1. Pressure outlets were placed at cystic duct outlet while velocity inlets were placed at the cystic duct inlet. The non-slip condition was employed throughout the lumen wall.

The cast geometry was discretised with tetrahedron cells. Grid independence checks were performed in all models. The basic number of cells was chosen to represent the shape of the flow domain without excessive truncation on the actual geometry while ensure a mesh independence of the numerical solution. The effect of mesh density variation was assessed by performing a series of simulations at different mesh densities until the flow parameters are independent of the mesh. The mesh was then further refined according to various local flow patterns at the critical flow regions, e.g. sudden contraction of the cystic duct neck where velocity and pressure gradients are high. Approximately 1.2 and 0.6 million cells were employed to discretise the flow structures to satisfaction in Cast010 and Cast034, respectively. The computational effort for solving the flow takes between 28 and 32 h of CPU time for each flow case.

4. Results and discussion

4.1. Flow structures

Flow patterns in the cystic duct models were visualised using path lines—trajectories of massless particles in the domain. Each individual path line was coloured spatially by velocity magnitude

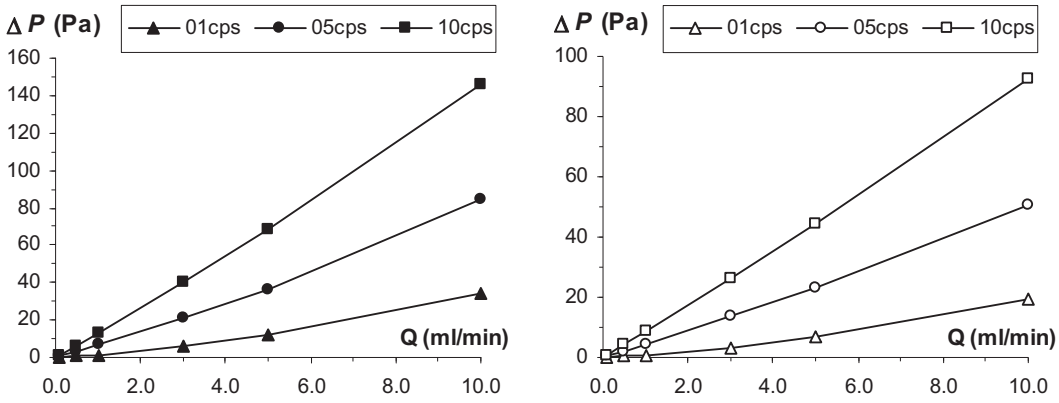

Fig. 5. Pressure difference across the cystic duct of Cast034 (left) and Cast010 (right).

($m\,s^{-1}$) contours to illustrate the acceleration or deceleration experienced by the particle in each trajectory. In addition, numbered cross-sectional planes were used to show local relative strength of the secondary flow.

To represent gallbladder emptying, the flow structures at two typical flow rates, 1 ml/min (average) and 5 ml/min (maximum) through Cast010 are is shown in Fig. 2. The cystic duct inlet is placed at pane-1. At a flow rate of 1 ml/min, it can be seen that the pathlines negotiates the duct geometry easily especially at the neck and the cystic duct's distal end (*pars glabra*) region. Fluid particles accelerate to the maximum velocity near plane-5 and slow down at plane-8 where the distal end of the cystic duct is situated.

Because of the curved nature of the cystic duct models, secondary flow is induced by the centrifugal forces. The higher the secondary flow, the higher is the pressure drop across the duct. At the flow rate of 1 ml/min, the maximum secondary velocity vector is 4.0E−3 $m\,s^{-1}$ compared to the 1.5E−2 $m\,s^{-1}$ maximum velocity magnitude. When the flow is increased to 5 ml/min, these values become 2.7E−2 and 7.0E−2, respectively, indicating stronger secondary flow. At larger flow, a pair of counter-rotating secondary flow cells was observed in plane-3, 4 and 6. The peak of the velocity contour in plane 5 was shifted away from the centre forming a saddle-like profile (Fig. 3).

Path lines plots of Cast034 are shown in Fig. 4. The bulk flow rate of 1 ml/min negotiates the helical arrangement smoothly. However, at 5 ml/min the flow appears to twist along its flow path. Fluid particles accelerate to the maximum velocity at plane-5 that has the minimum cross-sectional area.

When the flow rate is at 1 ml/min, the maximum velocity magnitude and secondary velocity is 2.37E−2 $m\,s^{-1}$ and 7.79E−4 $m\,s^{-1}$, respectively. As the flow rate increases to 5 ml/min, stronger secondary motion is observed and these values elevates to 1.05E−1 $m\,s^{-1}$ and 1.99E−2 $m\,s^{-1}$, respectively. At larger flow, single group of anti-clockwise secondary vectors were observed in plane-3, 4 and 5. The peak of the velocity magnitude contour in plane 5 was again shifted away from the plane centre forming a saddle profile.

4.2. Pressure drop

In order to assess the amount of "resistance" the cystic duct exerts against the flow of bile as the gallbladder empties, the pressure drop across the cystic ducts is computed. This pressure drop represents the difference between the pressure in the gallbladder and that at the exit of the cystic duct and it is the driving force for emptying the gallbladder. Under physiological conditions, the human bile viscosity, μ can vary from 1 to roughly 10 mPa s [2]. Therefore, three μ values (1, 5 and 10 mPa s) were used to estimate the pressure difference, ΔP across the cystic ducts for various flow rates, Q. These flow rates correspond to Reynolds numbers that range from 0.1 to 100 based on the average diameter of the cystic duct model. This is shown in Fig. 5. As expected, the pressure drop increases as the flow rate and the viscosity increase. The resulting pressure drop across the cystic duct is within the clinically recorded range.

Fig. 6 shows the relationship between Reynolds number and the friction factor (a) and the dimensionless pressure (b) for cystic ducts compared to a straight circular tube. Both figures are typical of laminar flow and they show a 4 times higher resistance to the flow in the cystic ducts when compared to an equivalent straight circular

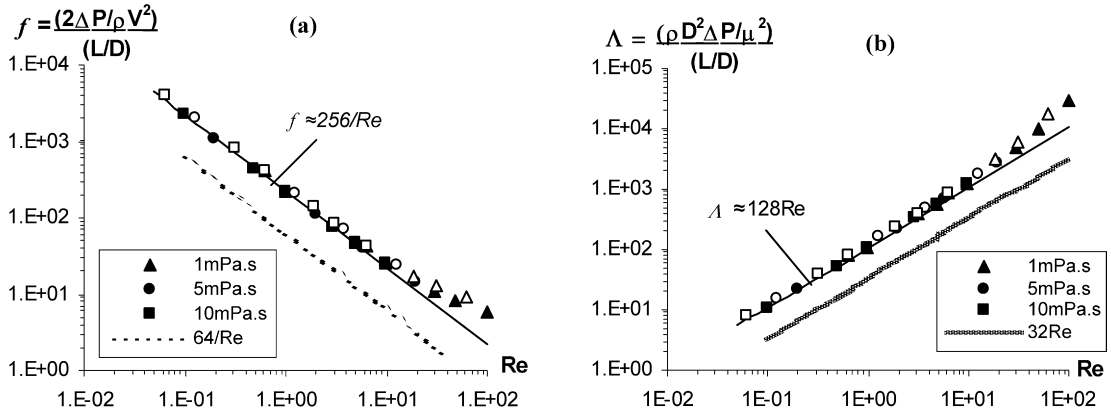

Fig. 6. Dimensionless plots: (a) f vs. Re and (b) Λ vs. Re.

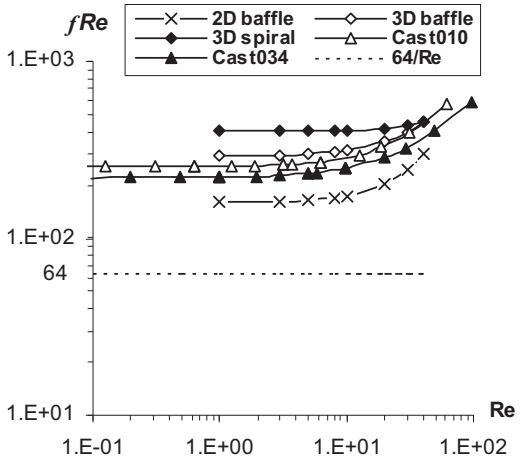

Fig. 7. Comparison of Ref plots between 3D casts models and idealised CD ducts with 10 baffle/spirals [2].

tube. The higher resistance can be attributed to the presence of the valves of Heister and it indicates higher resistance to the gallbladder emptying.

The friction factors for the cystic ducts decrease as the Reynolds number increases. This behaviour is characteristic of laminar flow condition and it continues up to Reynolds number of 40 above which the values of friction factors start to appear less dependent on the Reynolds number indicating somehow a transition towards a turbulent like flow. This behaviour is identical to that reported by Al-Atabi et al. [13] in their experimental study. This is an indication that the flow in the cystic duct within the physiological range (*Re* of 1–40) is indeed laminar.

Ooi et al. [2] performed extensive numerical analysis into the flow of bile in two-dimensional and three-dimensional idealised models of cystic duct. The idealised two-dimensional cystic duct model was represented by a channel with alternating baffles to represent the valves of Heister, while the three-dimensional duct was idealised as a circular tube with baffles or spirals to represent the valves of Heister. Fig. 7 shows the relationship between the Reynolds number (*Re*) and the product of the friction and Reynolds number and it compares the results reported by Ooi et al. [2] for the idealised cystic ducts to those of the realistic ones investigated in this study. The curves are generally horizontal at relatively low *Re* and begin to increase once past a critical *Re* in each case. The horizontal part of the curves actually represented the flow major loss dominant regime. The dimensionless term $Re\,f$ yields the numerator in the term $64/Re$ for straight pipe. As *Re* increases past their respective critical points, the *Re* dependent part resembles the flow regime where minor losses begin to become significant. The comparisons in Fig. 7 show the 3D models are close to the cast models with the idealised spiral duct showing highest resistance and least dependency on *Re*.

5. Conclusions

Numerical flow simulations in realistic cystic ducts have been performed. The geometries were generated from resin casts of real cystic ducts surgically removed from patients. These simulations are performed to obtain quantitative readings to compare with clinical measurements.

The results showed that dimensionless pressure drops across the cystic ducts are 4 times higher than those of a straight circular tube of an equivalent length and average diameter. This can be attributed to the convoluting nature of the studied cystic ducts, which resulted in strong secondary flow that contribute to higher losses. The absolute pressure drop across the cystic duct compared very well with those obtained from clinical observations. From the hydrodynamic point of view, the cystic duct lumen seems to serve as a passive resistor that strives to provide a constant amount of resistance. The good comparison between clinical observation and the CFD results is an indication that CFD is an appropriate tool to investigate the functions of the biliary system. Future work can include simulating the entire biliary system with both gallbladder filling and emptying including taking into consideration the compliance of the cystic duct's wall.

Conflict of interest statement

The authors declare that they have no conflict of interest.

References

[1] Shaffer EA. Control of gallbladder motor function. Alimentary Pharmacology and Therapeutics 2000;14:2–8.
[2] Ooi RC, Luo XY, Chin SB, Johnson AG, Bird NC. The flow of bile in the human cystic duct. Journal of Biomechanics 2004;37:1913–22.
[3] Liddle RA, Gerty BJ, Kanayam S, Beccaria L, Coker LD, Turnbull TA, et al. Effect of a novelcholecystokinin (CCK) receptor antagonist, MK-329, on gallbladder contraction and gastric emptying in humans. Journal of Clinical Investigation 1990;84:1220–2125.
[4] Calvert NW, Troy GP, Johnson AG. Laparoscopic cholecystectomy: a good buy? A cost comparison with small-incision (mini) cholecystectomy. European Journal of Surgery 2000;166:782–6.
[5] Holzbach RT, Marsh M, Olszewski M, Holan K. Evidence that supersaturated bile is frequent in healthy man. Journal of Clinical Investigation 1973;52:1467–79.
[6] Nakayama F, van der Linden W. Stratification of bile in gallbladder and gallstone formation. Surgery, Gynecology and Obstetrics 1975;141:587–90.
[7] Deenitchin GP, Yoshida J, Chijiiwa K, Tanaka M. Complex cystic duct is associated with cholelithiasis. HPB Surgery 1998;11:33–7.
[8] Jazrawi RP, Pazzi P, Petroni ML, Prandini N, Paul C, Adam JA, et al. Postprandial gallbladder motor function, Refilling and turnover of bile in health and in cholelithiasis. Gastroenterology 1995;109:582–91.
[9] Al-Atabi MT, Chin SB, Luo XY. Flow structure in circular tubes with segmental baffles. Journal of Flow Visualization and Image Processing (JFVIP) 2005;12(3):301–11.
[10] Al-Atabi MT, Chin SB, Luo XY. Visualization experiment of flow structures inside two-dimensional human biliary system models. Journal of Mechanics in Medicine and Biology (JMMB) 2006;6(3):249–60.
[11] Al-Atabi MT, Chin SB, Luo XY. Cystic duct visual-based evaluation of gallstones formation risk factors. Journal of Engineering Science and Technology (JESTEC) 2006;1(1):1–9.
[12] Al-Atabi MT, Chin SB, Luo XY, Beck SBM. Investigation of the flow in a compliant idealised human cystic duct. Journal of Biomechanical Science and Engineering 2008;3(3):411–8.
[13] Al-Atabi MT, Chin SB, Luo XY. Experimental investigation of the flow of bile in patient specific cystic duct models. ASME Journal of Biomechanical Engineering 2010;132(4).
[14] Li WG, Luo XY, Johnson AG, Hill NA, Bird N, Chin SB. One-dimensional models of the human biliary system. ASME Journal of Biomechanical Engineering 2007;129:164–73.
[15] Li WG, Luo XY, Chin SB, Hill NA, Johnson AG, Bird NC. Non-Newtonian bile flow in elastic cystic duct—one and three dimensional modelling. Annals of Biomedical Engineering 2008;36:1893–908.
[16] Li WG, Luo XY, Hill NA, Ogden RW, Smythe A, Majeed A, et al. Cross-bridge apparent rate constants of human gallbladder smooth muscle. Journal of Muscle Research and Cell Motility 2011;32:209–20.
[17] Li WG, Luo XY, Hill NA, Ogden RW, Smythe A, Majeed A, et al. Mechanical model for CCK induced acalculous gallbladder pain. Annals of Biomedical Engineering 2011;39:786–800.
[18] Heister L. A compendium of anatomy. London: Innys and Richardson; 1752.
[19] Mentzer SH. The valves of Heister. Archives of Surgery 1926;13:511–22.
[20] Lichtenstein ME, Ivy AC. The function of the valves of Heister. Surgery 1937;1:38–53.
[21] Bird NC, Ooi RC, Luo XY, Chin SB, Johnson AG. Investigation of the functional three-dimensional anatomy of the human cystic duct: a single helix? Clinical Anatomy 2006;19:528–34.
[22] Operation manual. Fluent 6.1; 1999.
[23] Dodds WJ, Groh WJ, Darweesh R, Lawson TL, Kishk S, Kern MK. Sonographic measurement of gallbladder volume. American Journal of Roentgenology 1985;145:1009–11.
[24] Howard PJ, Murphy GM, Dowling RH. Gallbladder emptying patterns in response to a normal meal in healthy subjects and patients with gallstones: ultrasound study. Gut 1991;32:1406–11.
[25] Dodds WJ, Hogan WJ, Geenen JE. Motility of the biliary system. In: Schultz SG, editor. Handbook of physiology: the gastrointestinal system, vol. 1. Bethesda, MD: American Physiological Society; 1989. p. 1055–101.

[26] Hallenbeck GA. Biliary and pancreatic intraductal pressures. In: Code CF, editor. Handbook of physiology, alimentary canal, secretion, section 6. Washington, DC: American Physiological Society; 1967. p. 1007–25.
[27] Macpherson BR, Scott GW, Chansouria JPN, Fisher AWF. The muscle layer of the canine gallbladder and cystic duct. Acta Anatomica 1984;120:117–22.
[28] Majeed AW, Smythe A, Johnson AG. Continuous ambulatory manometry of the human gallbladder. Internal Report. Academic Surgical Unit, the University of Sheffield; 2006.
[29] Johnston CG, Brown CE. Studies of gall-bladder function. III. A study of the alleged impediment in the cystic duct to the passage of fluids. Surgery. Gynaecology and Obstetrics 1932;54:477–85.
[30] Tanaka M, Ikeda S, Nakayama F. Change in bile duct pressure responses after cholecystectomy: loss of gallbladder as a pressure reservoir. Gastroenterology 1984;87:1154–9.